Exact Fisher zeros and thermofield dynamics across a quantum critical point

Yang Liu, Songtai Lv, Yuchen Meng, Zefan Tan, Erhai Zhao, ** and Haiyuan Zou 1,†

1 Key Laboratory of Polar Materials and Devices (MOE), School of Physics and Electronic Science,

East China Normal University, Shanghai 200241, China

2 Department of Physics and Astronomy, George Mason University, Fairfax, Virginia 22030, USA

(Received 8 July 2024; accepted 28 October 2024; published 14 November 2024)

By setting the inverse temperature β loose to occupy the complex plane, Fisher showed that the zeros of the complex partition function Z, if approaching the real β axis, reveal a thermodynamic phase transition. More recently, Fisher zeros were used to mark the dynamical phase transition in quench dynamics. It remains unclear, however, how Fisher zeros can be employed to better understand quantum phase transitions or the nonunitary dynamics of open quantum systems. Here we answer this question by a comprehensive analysis of the analytically continued one-dimensional transverse field Ising model. We exhaust all the Fisher zeros to show that in the thermodynamic limit they congregate into a remarkably simple pattern in the form of continuous open or closed lines. These Fisher lines evolve smoothly as the coupling constant is tuned, and a qualitative change identifies the quantum critical point. By exploiting the connection between Z and the thermofield double states, we obtain analytical expressions for the short- and long-time dynamics of the survival amplitude, including its scaling behavior at the quantum critical point. We point out Z can be realized and probed in monitored quantum circuits. The exact analytical results are corroborated by the numerical tensor renormalization group. We further show that similar patterns of Fisher zeros also emerge in other spin models. Therefore, the approach outlined may serve as a powerful tool for interacting quantum systems.

DOI: 10.1103/PhysRevResearch.6.043139

Introduction. There is a renewed interest in the concept of complex-valued partition function and its zeros in quantum many-body physics. In the seminal work of Lee and Yang on phase transitions, the magnetic field in spin Hamiltonians (or the chemical potential in a grand canonical ensemble) is analytically continued to take on complex values [1,2]. Then phase transitions in the thermodynamic limit can be inferred and analyzed by tracking the zeros of the complex-valued partition function Z evaluated for finite-size systems. Fisher extended the recipe by allowing the inverse temperature β = $1/k_BT$ to be complex instead, which applies to all systems [3]. Yet, compared to the Lee-Yang zeros, the Fisher zeros are more challenging to find or analyze. Because β couples to every term in the Hamiltonian, the locations of Fisher zeros on the complex β plane appear to feature less regularity. They may not form simple smooth curves as the thermodynamic limit is approached [4], in sharp contrast to the celebrated circle theorem for Lee-Yang zeros [1,2,5]. To unveil the unifying patterns behind the ostensible complexity of Fisher zeros, exact analytical results would be greatly helpful.

*Contact author: ezhao2@gmu.edu
†Contact author: hyzou@phy.ecnu.edu.cn

Published by the American Physical Society under the terms of the Creative Commons Attribution 4.0 International license. Further distribution of this work must maintain attribution to the author(s) and the published article's title, journal citation, and DOI.

Fisher zeros were invented to comprehend thermodynamic phase transitions. Recently, several of us [6] proposed to use them to probe quantum phase transitions [7]. Numerical data on the one-dimensional transverse field Ising model (1DT-FIM) reveal that as the coupling constant (the transverse field) g is tuned, the motion of certain Fisher zeros correlates with the energy gap associated with the domain wall excitations. The analysis of Ref. [6] was limited to $g \le 1$, so a natural question is what happens on the disordered side g > 1. Naively, one might expect from the Kramers-Wannier (KW) duality [8] that the zeros at g > 1 simply mirror those at g < 1. This conjecture turns out to be false. We shall show that the KW duality breaks down for complex β . To establish a correct, complete picture of Fisher zeros across the quantum critical point (QCP), an exact formula of Z valid for all g values is required to delineate the intricate interplay of quantum and thermal fluctuations in various regions of the complex β plane.

An even more significant impetus for complex Z comes from the flurry of experiments on quantum simulators and quantum circuits which prompted the generalization of the notion of phase transitions to time-dependent and open quantum systems [9]. The complex zeros of the Loschmidt echo amplitude were used to define dynamical phase transition in quench dynamics [10]. Following the discovery of measurement induced phase transitions in nonunitary quantum circuits [11–13], various non-Hermitian generalizations of the Ising model have been considered where the coupling constants become complex valued as a result of the nonunitary evolution introduced by measurements. For example, Ref. [14] mapped

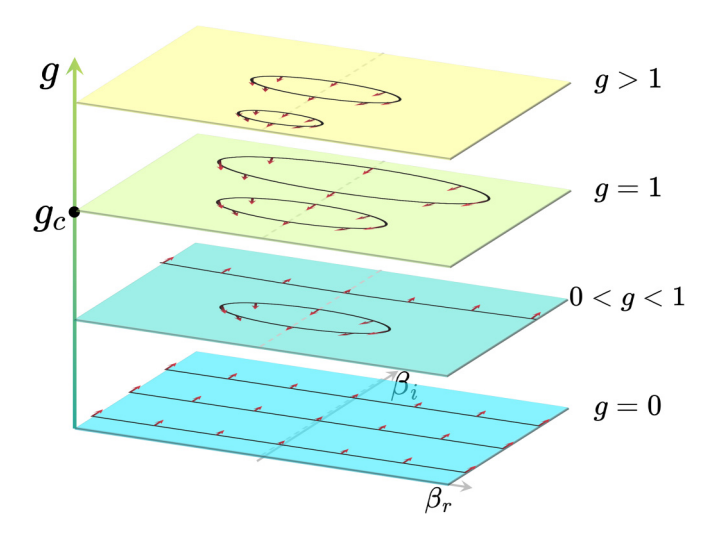


FIG. 1. The continuous lines of Fisher zeros on the complex $\beta = \beta_r + i\beta_i$ plane for 1DTFIM (schematic). The arrows indicate the velocities of the zeros as the transverse field g is increased. At g=0, the zeros congregate into a set of open lines. As g increases, closed lines (ovals) of zeros appear, while the open lines shift upwards to larger β_r and eventually vanish at the QCP ($g=g_c=1$). The closed lines continue to move toward the origin as g is further increased beyond g_c .

a nonunitary quantum circuit to a 2D classical Ising model at complex temperature. These developments hint a new era of complex Z in which the complexification is no longer just a mathematical trick but mandated by experiments to take on physical significance.

This work is inspired by the confluence of these ideas. By exhausting the Fisher zeros for a canonical quantum manybody system, the 1DTFIM, we describe how insights about quantum phase transitions and quantum dynamics can be gleaned from the complex-valued partition functions $Z(\beta)$. A few surprising results are obtained. (i) In the thermodynamic limit, the Fisher zeros of 1DTFIM form continuous curves (lines and loops) which move smoothly as the coupling constant g is tuned. (ii) Even though the Fisher zeros never touch the real β axis, the quantum critical point can be unambiguously inferred from either the vanishing of open lines (Fig. 1) or the scaling of low-energy excitations extracted from Z. (iii) We exploit the connection between Z and the maximally entangled thermofield double (TFD) states [15], which are dual to eternal black holes according to the AdS/CFT correspondence [16], to make analytical predictions about the dynamics of TFD. These include the short-time decay of the survival probability, its periodic oscillation at low temperatures, and the recurrence time at the quantum critical point. (iv) We further show that aside from being a useful theoretical device, Z can be realized and probed in nonunitary quantum circuits where the unitary evolution of the qubits is interspersed with projective measurements and post selection.

Fisher zeros from the exact partition function. The Hamiltonian of the 1DTFIM can be written as

$$H = -\sum_{i=1}^{L} \left(\sigma_i^z \sigma_{i+1}^z + g \sigma_i^x \right), \tag{1}$$

where σ_i^x and σ_i^z are the Pauli matrix operators on site i, and the coupling constant g is the transverse magnetic field measured in units of the nearest neighbor Ising interaction (set to one). As is well known, in the thermodynamic limit $(L \to \infty)$, a quantum phase transition at the critical coupling $g_c = 1$ separates the ferromagnetic phase (g < 1) from the paramagnetic phase (g > 1).

While 1DTFIM is exactly solvable, the analytical form of its partition function Z is subtle to write down. Usually the model is treated in fermionic representation after the Jordan-Wigner transformation, where one has to confront the two sectors of the total fermion number [17]. We find it cleaner to stick to the spin representation and map $Z = \text{Tr}e^{-\beta H}$ to that of an anisotropic 2D Ising model and its Onsager-Kaufman solution [18,19] by Trotter decomposition along the imaginary time axis β which plays the role of another spatial dimension γ [20]. The result is

$$Z = \frac{1}{2} \left[\prod_{k=1}^{L} 2 \cosh(\beta \epsilon_{2k}) + \text{sign}(g_c - g) \prod_{k=1}^{L} 2 \sinh(\beta \epsilon_{2k}) + \prod_{k=1}^{L} 2 \cosh(\beta \epsilon_{2k-1}) + \prod_{k=1}^{L} 2 \sinh(\beta \epsilon_{2k-1}) \right],$$
 (2)

where $\epsilon_k = [1 + g^2 - 2g\cos(\pi k/L)]^{1/2}$. We refer to Eq. (2) as the Suzuki solution, even though the all important $\operatorname{sign}(g_c - g)$ did not appear explicitly in Ref. [20] and perhaps is not widely appreciated. Without the sign factor, one would have expected the KW duality [8], i.e., Z is invariant under the transformation $g \to 1/g$, $\beta \to g\beta$ so that it is sufficient to analyze the subspace g < 1. This is only an illusion: the correct formula Eq. (2) shows that Z itself does not possess KW duality and implies the presence of the recently proposed noninvertible symmetry [21,22]. The distribution of Fisher zeros on the quantum disordered side g > 1 is qualitatively different from the ordered side g < 1. From the expression of Z, Fisher zeros can be located and visualized by following the procedure outlined in [23].

Tensor renormalization group with complex β . We also compute Z using an independent numerical method which serves two purposes. First, it confirms the analytical solution Eq. (2) is correct. Second, it demonstrates a general and precise technique to compute $Z(\beta \in \mathbb{C})$ for interacting quantum spin models for which there is no exact solution. Since Z can be represented as the trace of a product of local tensors, it can be evaluated by tensor network algorithms [24–26] which have proven to be efficient and accurate for spin models [27]. Starting from the 1D system, we first construct a 2D "lattice" of size $L \times N$ by Trotter decomposition $\beta = \tau N$. Then, Z is obtained from the high order tensor renormalization group (HOTRG) [28]. We have checked that tensor results are in agreement with both exact diagonalization and the exact solution above (see [23] for details).

It is worth to mention that when β is complex, Monte Carlo develops sign problems but HOTRG can yield Z accurately [27]. Previously, renormalization group (RG) transformation has been generalized to the complex β plane to study confinement in lattice gauge theory and classical O(N) models. It was observed that the Fisher zeros are located at the

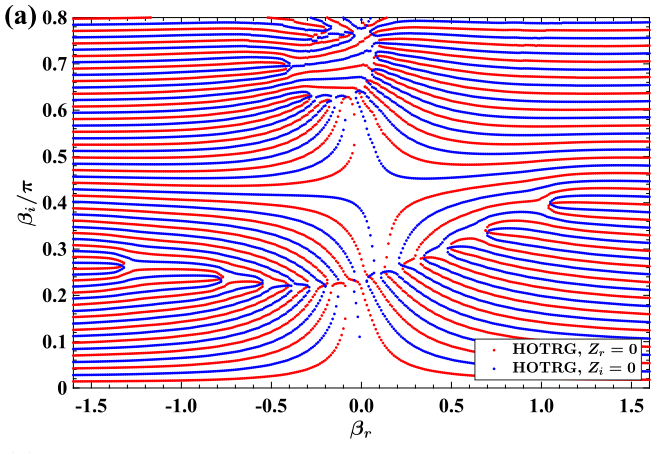
boundary of the attraction basins of infrared fixed points, and they control the global properties of the complex RG flows [29,30]. Here we confine our attention to the evaluation of Fisher zeros through HOTRG but for quantum spin models.

Motion of Fisher zeros across QCP. The exact solution corroborated by HOTRG yields a complete picture, sketched in Fig. 1, of the evolution of Fisher zeros on the complex β plane as the coupling constant g is varied. The main observations are summarized into (i)–(iv) below. (i) The Fisher zeros of 1DTFIM appear as continuous lines, rather than isolated points or densely packed regions, in the thermodynamic limit $L \to \infty$. (ii) For g < 1, there exist open lines of zeros that are approximately parallel to the β_r axis. (iii) As g increases from zero to one, these open lines shift upwards toward large β_i , and vanish completely at the QCP g = 1. (iv) Away from g = 0, closed loops of Fisher zeros also appear and persist for all g. These loops are centered around the β_i axis and move toward $\beta_i = 0$ as g is increased. We stress that properties (i)-(iv) came as surprises, in the sense that they are not obvious from staring at the model or the exact solution

Some of these features can be appreciated by considering a few limit cases. At g = 0, $Z = \text{Tr}V^L$ where the transfer matrix $V = e^{\beta} + \sigma_x e^{-\beta}$. The Fisher zeros are determined by the condition $\tanh \beta = e^{in\pi/L}$ with n an integer, i.e., they are uniformly distributed on the unit circle on the plane of tanh β [14]. On the complex β plane, the zeros form a set of straight lines at $\beta_i = \pi/4 + m\pi/2$, with m an integer, as $L \to \infty$. Another simple case is the small size system with L=2. After some algebra, one finds the zeros are located on the β_i axis at $\beta_i = (m + \frac{1}{2})\pi/(\sqrt{1+g^2\pm 1})$ where m again is an integer. While the size L=2 is too small to feature Fisher zeros away from the β_i axis or the closed loops, it does correctly capture the trend that the zeros move toward $\beta_i = 0$ as g is increased. We note that previous work [31] focused on zeros on the imaginary β axis originated from the cosh terms in Z.

It is clear from (iii) that the QCP is marked by a qualitative change in the Fisher zeros. To describe the lowest open Fisher line, one can take its imaginary part β_i at some fixed large value of β_r and plot $1/\beta_i$ against g. In Ref. [6], it was shown that the resulting curve is linear near QCP. Similarly, for the closed Fisher lines, we can select a characteristic point on each curve, e.g., the β_i value of the rightmost point. Then a linear relationship between $1/\beta_i$ and g is observed on the disordered side g > 1, which is consistent with the spin flip excitations. A more refined description is to define the velocities of the zeros on the complex β plane with increasing g. Interestingly, we find the speed of the zeros exhibits properties similar to the Grüneisen parameter [32,33], see [23].

Fisher zeros in other spin models. We conjecture that the regularity of Fisher's zeros and its correlation with QCP, observed above for 1DTFIM, generalize to a host of other systems. Since Z and its zeros can be reliably computed from the tensor network method, the program outlined here can serve as a powerful diagnostic tool for quantum many-body physics. To illustrate this, we consider two examples. The first is the axial next nearest neighbor Ising (ANNNI) model with



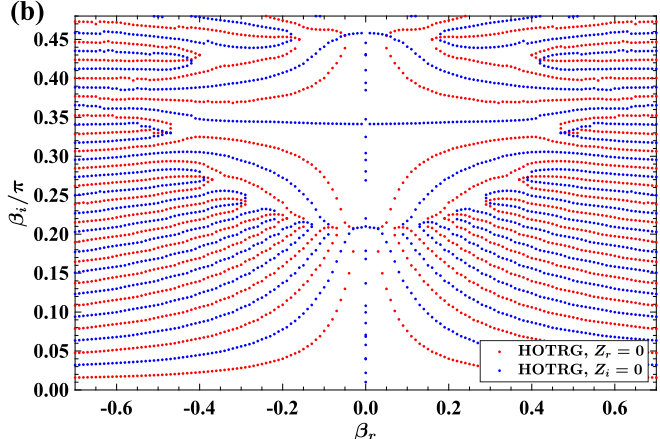


FIG. 2. The pattern of Fisher zeros, as the intersections of $Z_r = 0$ (red) and $Z_i = 0$ (blue) computed by HOTRG for finite-size systems (L = 32), on the complex β plane. (a) The zeros for the ANNNI model with $\kappa = 0.1$ and g = 0.5, calculated with D bond $D_b = 30$, form an open line near the β_r axis. (b) In the XY model with $\gamma = 0.01$, calculated with $D_b = 50$, the zeros near the β_r axis form closed loops.

the Hamiltonian

$$H = -\sum_{i=1}^{L} \left(\sigma_i^z \sigma_{i+1}^z - \kappa \sigma_i^z \sigma_{i+2}^z + g \sigma_i^x \right),$$

where we choose $\kappa = 0.1$ and g = 0.5 so the system has a gap. The second is the XY model with the Hamiltonian

$$H = \sum_{i=1}^{L} \left[(1+\gamma)\sigma_{i}^{x}\sigma_{i+1}^{x} + (1-\gamma)\sigma_{i}^{y}\sigma_{i+1}^{y} \right],$$

where we chose $\gamma=0.01$, bringing the system close to a QCP. For both systems, numerical calculations show that as L increases, the zeros indeed approach continuous lines. Figure 2 compares the Fisher zeros of these two models obtained from HOTRG with L=32 [23]. For the ANNNI model, open lines corresponding to domain wall excitations still exist. But the zero locations are no longer symmetric between $\beta_r>0$ and $\beta_r<0$, causing the open lines to tilt. For the XY model near QCP, we witness a similar qualitative change as seen in the 1DTFIM: the open lines completely vanish, giving way to closed loops. The change is mandatory because otherwise, the

two phases separated by the QCP would share the same global patterns of RG flows on the complex β plane, which would contradict the fact that they correspond to different RG fixed points.

What can Z tell us about quantum dynamics? We now view Z from another perspective, as the survival amplitude of a certain quantum state. Let $\beta = \beta_r + it$, and interpret the imaginary (real) part of β as time t (the inverse temperature $\beta_r = 1/k_BT$). Let E_n be the eigenenergies, and $|n\rangle$ the corresponding eigenstates. Then

$$Z(\beta_r, t) = \sum_{n} e^{-\beta_r E_n} e^{-iE_n t}$$

describes the unitary dynamics of a mixed ensemble. The modulus square of Z defines the spectral form factor

$$S(\beta_r, t) = \left| \frac{Z(\beta_r, t)}{Z(\beta_r, 0)} \right|^2,$$

which is normalized to 1 as t = 0. The disorder average of S has been used to diagnose chaos and information scrambling in Hamiltonians containing random couplings, e.g., the SYK model [34]. Following Ref. [35], we purify the mixed state above by introducing the thermofield double state in an enlarged Hilbert space

$$|\psi(\beta_r,0)\rangle = \frac{1}{\sqrt{Z(\beta_r,0)}} \sum_n e^{-\beta_r E_n/2} |n\rangle_L \otimes |n\rangle_R,$$

where, for clarity, the subscripts L, R are used to denote the left and right copy, respectively [15]. Under the single Hamiltonian $H_L \otimes 1_R$, the TFD state evolves with time as $\psi(\beta_r, t) = e^{-it(H_L \otimes 1_R)} |\psi(\beta_r, 0)\rangle$. One finds that S is nothing but the survival probability [35]

$$S(\beta_r, t) = |\langle \psi(\beta_r, t) | \psi(\beta_r, 0) \rangle|^2$$
.

In contrast to the Loschmidt echo in quench dynamics [10], here the connection between *Z* and quantum dynamics is established by the TFD states, which are dual to the eternal black hole in the context of AdS/CFT correspondence [16]. Via this bridge, the detailed knowledge about the analytical structure of *Z*, including the Fisher zeros, can now be translated into new insights about quantum dynamics. Three examples for the 1DTFIM are given below.

The short time dynamics of S is characterized by exponential decay $S(t) \simeq e^{-(t/\tau)^2}$ with $\tau^2 = k_B \beta_r / C_V$. Figure 3(a) shows the specific heat capacity C_V/L obtained by fitting S(t) at some typical values of g. The decay rate $1/\tau \propto \sqrt{C_V}$ correlates with the locations of Fisher zeros at which S is forced to vanish. This can be seen on the low β_r portion of Fig. 3(a): as g is increased from g=1, the Fisher zeros move closer to the β_r axis, and accordingly S is suppressed from one to zero at an increasing rate. At high β_r , however, the decay is most rapid at the QCP, where quantum fluctuation is strong and C_V reaches maximum.

The long time behavior of S(t) is complicated but simplicity emerges at low temperatures. To understand this, we can convert the products of hyperbolic sines and cosines in the exact solution of Z into sums and expand them for large β_r . The leading contributions to S(t) are

$$S(t) \simeq 1 + 2e^{-\beta_r \Delta} \cos(\Delta t) + ...,$$

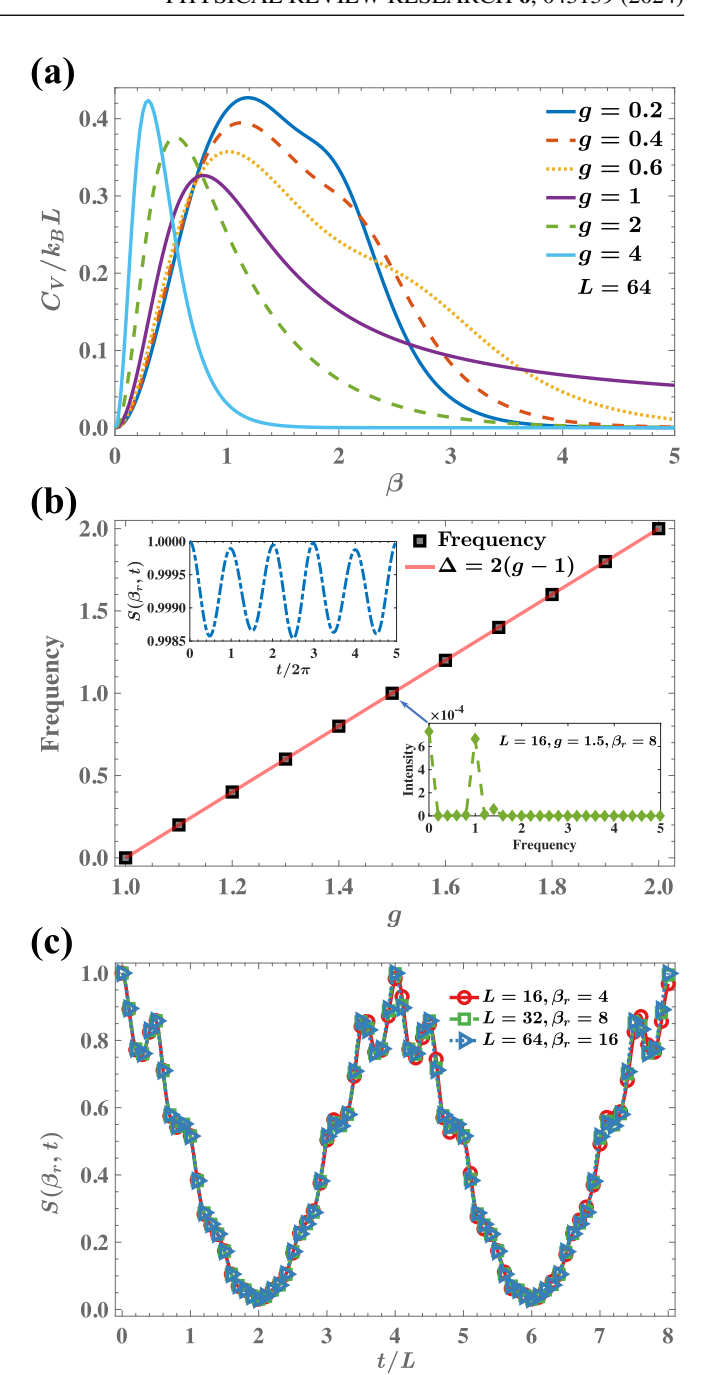


FIG. 3. The rich behaviors of the spectral form factor (survival probability) $S(\beta_r, t)$. (a) The short-time decay of S is dictated by the specific heat capacity C_V/L . (b) The low temperature oscillations (inset, g=1.5) of S. The oscillation frequency obtained from Fourier transform can be fit by $\Delta=2(g-1)$ and vanishes at QCP. (c) Fine structures of S over long time scales for different β_r and L. At the QCP, all exhibit the same periodicity $t^*=4L$. The overlay of curves shows self-similarity, $S(\beta_r, t)_L \approx S(n\beta_r, nt)_{nL}$ with n=2.

where the oscillation frequency $\Delta = \sum_k (\epsilon_{2k-1} - \epsilon_{2k})$ has the meaning of the excitation gap. Previously in Ref. [6], it was noted from numerics that for $g \le 1$ the oscillation frequency vanishes at the QCP while the oscillation amplitude reaches maximum. The analytic asymptote derived here not only explains this observation but also expands its validity to the

disordered side $g \ge 1$ [Fig. 3(b)]. Thus, the low temperature oscillations of $Z(\beta_r, t)$ provide another diagnostic tool for QCP.

The dynamics of S exhibits rich scaling behaviors at the QCP. For a system of finite size L, the energy spectrum is discrete and the initial TFD state will come back to itself after the quantum recurrence time t^* . To find t^* , take the limit of large β_r , expand the exact Suzuki solution, and carry out the k sum, we find at g = 1 the oscillation frequency is $\Delta = 2 \tan(\pi/4L)$ which becomes $\pi/2L$ in the limit of large L to yield $t^* = 4L$. For smaller β_r , S(t) deviates significantly from the sinusoidal form to acquire fine structures, but t^* stays approximately the same [23]. Our prediction $t^* = 4L$ agrees with the conformal field theory result from Ref. [17] (see [23] for details). We also observe that S exhibits self-similarity, i.e., $S(\beta_r, t)_L \approx S(n\beta_r, nt)_{nL}$ with n an integer, at the QCP and for intermediate to large (β_r, t) . Figure 3(c) shows an example with n = 2. This is consistent with the notion of criticality and provides a nice way to define RG flow in the complex plane (see [23] for details).

Probing Z from monitored quantum circuits. Lastly, we show that Z is not just a formal theoretical construct, it can be realized and probed in quantum circuits. Consider an array of qubits, j = 1, 2, ..., L. The standard single- and two-qubit Pauli gates implement unitary evolution such as $U_{77}(t) =$ $\exp(it\sum_i \sigma_i^z \sigma_{i+1}^z)$ and $U_x(t) = \exp(itg\sum_i \sigma_i^x)$. Let us define the cycle operator $U_F(t) = U_{zz}(t)U_x(t)$, then repeated application of U_F produces the time evolution corresponding to the 1DTFIM Hamiltonian, albeit in discretized form U(t) = $[U_F(t/N)]^N$. Now let us introduce nonunitary gates in the form of $U_x(i\beta_r)$ and $U_{zz}(i\beta_r)$, i.e., by replacing t with the imaginary time $i\beta_r$. These gates can be realized by including ancilla qubits and performing projective measurements and postselection on the ancilla [36–38], where the value of β_r characterizes the strength of the measurement. If we intersperse these unitary and nonunitary gates [9], e.g., by forming a cycle

$$U_F(\beta_r, t) = U_X(i\beta_r)U_X(t)U_{zz}(i\beta_r)U_{zz}(t),$$

the resulting evolution operator yields exactly $Z(\beta_r, t) = [U_F(\beta_r/N, t/N)]^N$ in the limit of large N. From this perspective, $Z(\beta_r, t)$ describes the competition between unitary time evolution and quantum measurement in an open quantum many-body system.

The circuit construction here differs from the approach in Ref. [14] based on the transfer matrix. From an alternative perspective, the nonunitary gates introduce imaginary parts to the coupling constants in the Hamiltonian and render it non-Hermitian [39]. Previous studies on non-Hermitian Ising-type models mostly focused on their entanglement or spectral properties [36–38]. Given the recent success in observing Lee-Yang zeros [40] and Loschmidt ratios [41], it seems promising that the circuit connection to *Z* and TFD states [42] can lead to future experimental studies of Fisher zeros [43].

Conclusion. In summary, we have presented a comprehensive analysis of the Fisher zeros in the 1DTFIM. We have demonstrated that Fisher zeros form continuous, smoothly shifting curves in the complex β plane, and they offer insights into quantum criticality despite never touching the real β axis. The complex partition function Z provides valuable analytical predictions about the quantum dynamics which is beyond the reach of the traditional thermodynamics, and can be realized and probed in nonunitary quantum circuits. Our clarification of the original Suzuki solution correctly captures the different excitations on the two sides of the QPT and the breakdown of the Kramers-Wannier duality. Successful generalization of the numerical analysis to other (the ANNNI and XY) spin models demonstrates that this approach can open up a promising avenue to study quantum critical systems in 1D [44-46] and higher dimensions [47–49].

Acknowledgments. We thank Youjin Deng, Shijie Hu, Ian McCulloch, Yannick Meurice, Tao Xiang, and Jiahao Yang for helpful discussions. This work is supported by the National Natural Science Foundation of China (Grant No. 12274126). E.Z. acknowledges the support from NSF Grant PHY-206419, and AFOSR Grant FA9550-23-1-0598.

C. N. Yang and T. D. Lee, Statistical theory of equations of state and phase transitions. i. theory of condensation, Phys. Rev. 87, 404 (1952).

^[2] T. D. Lee and C. N. Yang, Statistical theory of equations of state and phase transitions. ii. lattice gas and ising model, Phys. Rev. 87, 410 (1952).

^[3] M. Fisher and W. Brittin, Statistical Physics, Weak Interactions, Field Theory, Lectures in Theoretical Physics (University of Colorado Press, Boulder, 1965), Vol. VII C.

^[4] I. Bena, M. Droz, and A. Lipowski, Statistical mechanics of equilibrium and nonequilibrium phase transitions: The Yang-Lee formalism, Int. J. Mod. Phys. B 19, 4269 (2005).

^[5] T. Kist, J. L. Lado, and C. Flindt, Lee-Yang theory of criticality in interacting quantum many-body systems, Phys. Rev. Res. 3, 033206 (2021).

^[6] Y. Liu, S. Lv, Y. Yang, and H. Zou, Signatures of quantum criticality in the complex inverse temperature plane, Chin. Phys. Lett. 40, 050502 (2023).

^[7] S. Sachdev, *Quantum Phase Transitions* (Cambridge University Press, Cambridge, 2011).

^[8] H. A. Kramers and G. H. Wannier, Statistics of the twodimensional ferromagnet. part i, Phys. Rev. **60**, 252 (1941).

^[9] M. P. Fisher, V. Khemani, A. Nahum, and S. Vijay, Random quantum circuits, Annu. Rev. Condens. Matter Phys. 14, 335 (2023).

^[10] M. Heyl, A. Polkovnikov, and S. Kehrein, Dynamical quantum phase transitions in the transverse-field ising model, Phys. Rev. Lett. 110, 135704 (2013).

^[11] Y. Li, X. Chen, and M. P. A. Fisher, Quantum zeno effect and the many-body entanglement transition, Phys. Rev. B 98, 205136 (2018).

^[12] B. Skinner, J. Ruhman, and A. Nahum, Measurement-induced phase transitions in the dynamics of entanglement, Phys. Rev. X 9, 031009 (2019).

^[13] A. Chan, R. M. Nandkishore, M. Pretko, and G. Smith, Unitaryprojective entanglement dynamics, Phys. Rev. B 99, 224307 (2019).

- [14] S. Basu, D. P. Arovas, S. Gopalakrishnan, C. A. Hooley, and V. Oganesyan, Fisher zeros and persistent temporal oscillations in nonunitary quantum circuits, Phys. Rev. Res. 4, 013018 (2022).
- [15] Y. Takahashi and H. Umezawa, Thermo field dynamics, Int. J. Mod. Phys. B 10, 1755 (1996).
- [16] J. Maldacena, Eternal black Holes in anti-de Sitter, J. High Energy Phys. 04 (2003) 021.
- [17] Nivedita, H. Shackleton, and S. Sachdev, Spectral form factors of clean and random quantum ising chains, Phys. Rev. E **101**, 042136 (2020).
- [18] L. Onsager, Crystal statistics. i. a two-dimensional model with an order-disorder transition, Phys. Rev. 65, 117 (1944).
- [19] B. Kaufman, Crystal statistics. ii. partition function evaluated by spinor analysis, Phys. Rev. 76, 1232 (1949).
- [20] M. Suzuki, Relationship between d-dimensional quantal spin systems and (d + 1)-dimensional ising systems: Equivalence, critical exponents and systematic approximants of the partition function and spin correlations, Prog. Theor. Phys. **56**, 1454 (1976).
- [21] N. Seiberg and S.-H. Shao, Majorana chain and Ising model -(non-invertible) translations, anomalies, and emanant symmetries, SciPost Phys. 16, 064 (2024).
- [22] T. Senthil, Symmetries without an inverse: An illustration through the 1+1-D Ising model, Journal Club for Condensed Matter Physics (2024), doi:10.36471/JCCM_February_2024_ 03.
- [23] See Supplemental Material at http://link.aps.org/supplemental/ 10.1103/PhysRevResearch.6.043139 for (i) Discussion on the Suzuki solution, (ii) structure of Fisher zeros, (iii) Comparing the Suzuki solution and CFT at the quantum critical point, and (iv) self-similarity of *S*.
- [24] R. Orús, A practical introduction to tensor networks: Matrix product states and projected entangled pair states, Ann. Phys. 349, 117 (2014).
- [25] J. I. Cirac, D. Pérez-García, N. Schuch, and F. Verstraete, Matrix product states and projected entangled pair states: Concepts, symmetries, theorems, Rev. Mod. Phys. 93, 045003 (2021).
- [26] Y. Meurice, R. Sakai, and J. Unmuth-Yockey, Tensor lattice field theory for renormalization and quantum computing, Rev. Mod. Phys. 94, 025005 (2022).
- [27] A. Denbleyker, Y. Liu, Y. Meurice, M. P. Qin, T. Xiang, Z. Y. Xie, J. F. Yu, and H. Zou, Controlling sign problems in spin models using tensor renormalization, Phys. Rev. D 89, 016008 (2014).
- [28] Z. Y. Xie, J. Chen, M. P. Qin, J. W. Zhu, L. P. Yang, and T. Xiang, Coarse-graining renormalization by higher-order singular value decomposition, Phys. Rev. B 86, 045139 (2012).
- [29] A. Denbleyker, D. Du, Y. Liu, Y. Meurice, and H. Zou, Fisher's zeros as the boundary of renormalization group flows in complex coupling spaces, Phys. Rev. Lett. **104**, 251601 (2010).
- [30] Y. Meurice and H. Zou, Complex renormalization group flows for 2d nonlinear o(n) sigma models, Phys. Rev. D 83, 056009 (2011).
- [31] J. Liu, S. Yin, and L. Chen, Imaginary-temperature zeros for quantum phase transitions, Phys. Rev. B **110**, 134313 (2024).
- [32] L. Zhang, Universal thermodynamic signature of self-dual quantum critical points, Phys. Rev. Lett. 123, 230601 (2019).

- [33] L. Zhang and C. Ding, Finite-size scaling theory at a self-dual quantum critical point, Chin. Phys. Lett. **40**, 010501 (2023).
- [34] J. S. Cotler, G. Gur-Ari, M. Hanada, J. Polchinski, P. Saad, S. H. Shenker, D. Stanford, A. Streicher, and M. Tezuka, Black holes and random matrices, J. High Energy Phys. 05 (2017) 118.
- [35] A. del Campo, J. Molina-Vilaplana, and J. Sonner, Scrambling the spectral form factor: Unitarity constraints and exact results, Phys. Rev. D 95, 126008 (2017).
- [36] E. Granet, C. Zhang, and H. Dreyer, Volume-law to area-law entanglement transition in a nonunitary periodic gaussian circuit, Phys. Rev. Lett. 130, 230401 (2023).
- [37] V. Ravindranath and X. Chen, Robust oscillations and edge modes in nonunitary floquet systems, Phys. Rev. Lett. 130, 230402 (2023).
- [38] L. Su, A. Clerk, and I. Martin, Dynamics and phases of nonunitary floquet transverse-field ising model, Phys. Rev. Res. 6, 013131 (2024).
- [39] C. M. Bender and S. Boettcher, Real spectra in non-Hermitian Hamiltonians having *PT* symmetry, Phys. Rev. Lett. 80, 5243 (1998).
- [40] X. Peng, H. Zhou, B.-B. Wei, J. Cui, J. Du, and R.-B. Liu, Experimental observation of Lee-Yang zeros, Phys. Rev. Lett. 114, 010601 (2015).
- [41] P. Jurcevic, H. Shen, P. Hauke, C. Maier, T. Brydges, C. Hempel, B. P. Lanyon, M. Heyl, R. Blatt, and C. F. Roos, Direct observation of dynamical quantum phase transitions in an interacting many-body system, Phys. Rev. Lett. 119, 080501 (2017).
- [42] D. Zhu, S. Johri, N. M. Linke, K. Landsman, C. Huerta Alderete, N. H. Nguyen, A. Matsuura, T. Hsieh, and C. Monroe, Generation of thermofield double states and critical ground states with a quantum computer, Proc. Natl. Acad. Sci. 117, 25402 (2020).
- [43] B.-B. Wei, S.-W. Chen, H.-C. Po, and R.-B. Liu, Phase transitions in the complex plane of physical parameters, Sci. Rep. 4, 5202 (2014).
- [44] X. Chen, Z.-C. Gu, Z.-X. Liu, and X.-G. Wen, Symmetry protected topological orders and the group cohomology of their symmetry group, Phys. Rev. B **87**, 155114 (2013).
- [45] H. Zou, E. Zhao, X.-W. Guan, and W. V. Liu, Exactly solvable points and symmetry protected topological phases of quantum spins on a zig-zag lattice, Phys. Rev. Lett. 122, 180401 (2019).
- [46] Q. Zheng, X. Li, and H. Zou, Symmetry-protected topological phase transitions and robust chiral order on a tunable zigzag lattice, Phys. Rev. B **101**, 165131 (2020).
- [47] Z. Zhu, D. A. Huse, and S. R. White, Unexpected *z*-direction ising antiferromagnetic order in a frustrated spin- $1/2 J_1 J_2 xy$ model on the honeycomb lattice, Phys. Rev. Lett. **111**, 257201 (2013).
- [48] W.-Y. Liu, S.-S. Gong, Y.-B. Li, D. Poilblanc, W.-Q. Chen, and Z.-C. Gu, Gapless quantum spin liquid and global phase diagram of the spin- $1/2 J_1$ - J_2 square antiferromagnetic Heisenberg model, Sci. Bull. **67**, 1034 (2022).
- [49] H. Zou, F. Yang, and W. Ku, Nearly degenerate ground states of a checkerboard antiferromagnet and their Bosonic interpretation, Sci. China Phys. Mech. Astron. **67**, 217211 (2024).